JOURNAL OF AGRICULTURAL AND FOOD CHEMISTRY

Novel Online Sensor Technology for Continuous Monitoring of Milk Coagulation and Whey Separation in Cheesemaking

COLETTE C. FAGAN,*,† MANUEL CASTILLO,‡ FRED A. PAYNE,‡ COLM P. O'DONNELL,† MEGAN LEEDY,‡ AND DONAL J. O'CALLAGHAN§

Biosystems Engineering, UCD School of Agriculture, Food Science and Veterinary Medicine, University College Dublin, Earlsfort Terrace, Dublin 2, Ireland; Department of Biosystems and Agricultural Engineering, 128 C. E. Barnhart Building, University of Kentucky, Lexington, Kentucky 40546-0276; and Moorepark Food Research Centre, Teagasc, Fermoy, Co. Cork, Ireland

The cheese industry has continually sought a robust method to monitor milk coagulation. Measurement of whey separation is also critical to control cheese moisture content, which affects quality. The objective of this study was to demonstrate that an online optical sensor detecting light backscatter in a vat could be applied to monitor both coagulation and syneresis during cheesemaking. A prototype sensor having a large field of view (LFV) relative to curd particle size was constructed. Temperature, cutting time, and calcium chloride addition were varied to evaluate the response of the sensor over a wide range of coagulation and syneresis rates. The LFV sensor response was related to casein micelle aggregation and curd firming during coagulation and to changes in curd moisture and whey fat contents during syneresis. The LFV sensor has potential as an online, continuous sensor technology for monitoring both coagulation and syneresis during cheesemaking.

KEYWORDS: Optical sensor; light backscatter; coagulation; syneresis; curd moisture; whey fat; calcium chloride; temperature; cutting time

INTRODUCTION

There is currently a drive toward continuous monitoring and automation in the cheese-processing industry. Control of manufacturing processes through real time analysis of critical quality parameters can improve product quality and consistency. Full automation of the cheese manufacturing process is dependent on the development of technologies for monitoring unit operations, which affect final cheese quality. Cheese manufacture can be divided into a number of processing steps: milk coagulation in which casein micelles are destabilized and form a gel; syneresis during which whey is expelled from curd particles upon cutting of the gel; followed by drainage, molding, pressing, salting, and ripening of curd. Syneresis is a critical phase in cheese manufacture, with the rate and extent of syneresis playing a fundamental role in determining the moisture, mineral, and lactose content of drained curd and hence that of the final cheese (*1, 2*). Daviau et al. (*3*) stated that control of whey expelled during cheesemaking, including the control of syneresis in the vat, was a crucial step in cheese processing as the moisture content of the curd at the drainage step influenced the quality of the final product.

Obtaining a measurement of syneresis, which can be used to study and monitor the syneresis process, poses a number of difficulties as highlighted by the numerous and varied techniques that have been employed. A review of these techniques has been provided by Walstra et al. (*4*). The majority of techniques developed can be classed as either separation or dilution methods. In separation methods, curd and whey are separated and analyzed for curd moisture content or volume of whey, etc., to provide a measure of syneresis (*1, 5, 6*). However, Lawrence (*7*) demonstrated a difficulty with separation techniques. He found that the rate of syneresis was affected by the volume of whey which surrounded curd particles and that after the removal of curd from whey, there was a substantial increase in the rate of syneresis. The extent of this rapid expulsion of whey following separation is determined by the strength of curd particles. Therefore, a number of authors have explored the potential of a dilution technique to monitor syneresis. Such techniques aim to monitor syneresis with the curd remaining in the whey by using tracer molecules, which remain in the whey and are therefore diluted during syneresis (*8, 9*). Zviedrans and Graham (*8*) followed the progressive dilution of Blue Dextran 2000 in whey and found that it gave a reasonable estimate of the volume of whey expelled. However, it must be ensured that the tracer selected does not interfere with syneresis and/or adsorb to the curd grains. Indeed, the industrial use of markers to trace syneresis is prohibited by food safety regulations. Thus, this

* Corresponding author (telephone +353 1 7165541; fax +353 1 4752119; e-mail colette.fagan@ucd.ie).
† University College Dublin.
‡ University of Kentucky.
§ Moorepark Food Research Centre.

10.1021/jf070807b CCC: $37.00
Published on Web 09/14/2007

Table 1. Experimental Factors and Levels Employed in the Central Composite Rotatable Experimental Design

factor (coded value)	temperature (°C)	added $CaCl_2$ (mM)	cutting time[a] (β) (dimensionless)
−1.682	23.6	0.318	1.32
−1	27.0	1.00	1.80
0	32.0	2.00	2.50
1	37.0	3.00	3.20
1.682	40.4	3.68	3.68

[a] Experimental cutting time levels were selected as βt^*_{max}, where t^*_{max} was the time from enzyme addition to the inflection point of the light backscatter profile obtained using the CoAguLite sensor.

monitoring method is useful only in laboratory work. It is clear that neither separation nor dilution techniques are suitable to monitor online syneresis, rapidly and nondestructively, in a commercial setting. Recently a small number of studies have investigated techniques that may be adapted to the noninvasive monitoring of syneresis (*10, 11*). Taifi et al. (*10*) utilized an ultrasonic technique to monitor syneresis. They found syneresis was characterized by a large increase in attenuation of an ultrasound wave. An added advantage of using such a technique is its potential to be adapted to monitor both coagulation and syneresis. However, this study investigated the spontaneous onset of microsyneresis rather than syneresis as induced in industry by cutting a gel. An additional limitation of this technology would be the potential differences in ultrasound propagation through a mixture of curd and whey, as compared to that typically encountered in a homogeneous material such as a milk gel. The objective of this study was to determine if an optical sensor, having a large field of view relative to curd particle size and detecting light backscatter in a laboratory scale vat, could be applied to monitor both coagulation and syneresis during cheesemaking.

MATERIALS AND METHODS

Experimental Design. A three-factor, fully randomized, spherical, central composite design (CCD) was employed to evaluate the response of the proposed syneresis sensor prototype over a wide range of coagulation and syneresis rates. The CCD consisted of a 2^k factorial ($k = 3$) with $2k$ axial points and 6 center points (i.e., 20 runs in total) and was carried out in triplicate. The three factors selected as independent variables were coagulation temperature (T), calcium chloride ($CaCl_2$) addition level (CCAL), and cutting time (t_{cut}). The experimental factors, their selected levels, and coded values are presented in **Table 1**. Online, continuous monitoring of milk coagulation and curd syneresis in a 7 L cheese vat was performed using two different light backscatter sensor technologies, the CoAguLite (CL) and the Large Field of View (LFV) sensors. Light backscatter response from both sensors was continuously monitored from the time of rennet addition ($t_{c(0)}$) to the end of syneresis ($t_{s(85)}$). Experimental cutting time levels were selected by light backscatter measurements using the CL sensor as described below. The CL sensor also provided a reference light backscatter measurement to which the LFV sensor response could be compared in order to determine the LFV sensors ability to monitor coagulation and syneresis.

Milk Preparation and Compositional Analysis. Unpasteurized and unhomogenized milk was obtained from a local Kentucky milk-processing plant. Milk was pasteurized at 65 °C for 30 min and rapidly cooled to 2 °C. A 40 mL sample of milk was removed for compositional analysis, using a MilkoScan FT 120 (Foss Electric), and a further 7.20 kg of the milk was weighed for use in each experiment. $CaCl_2$ at the required level was added to the 7.20 kg of milk, stirred for 3 min, and then left to equilibrate for 30 min in a cold room at 2 °C. Milk was adjusted in the cold room to a pH of 6.51 using an experimentally obtained linear regression between 1.0 M HCl and pH to determine the volume of acid to add. The milk was stored in the cold room overnight. Milk pH adjustment after $CaCl_2$ addition ensured that any observed effect of calcium level on dependent variables was not due to an indirect effect of $CaCl_2$ on milk pH.

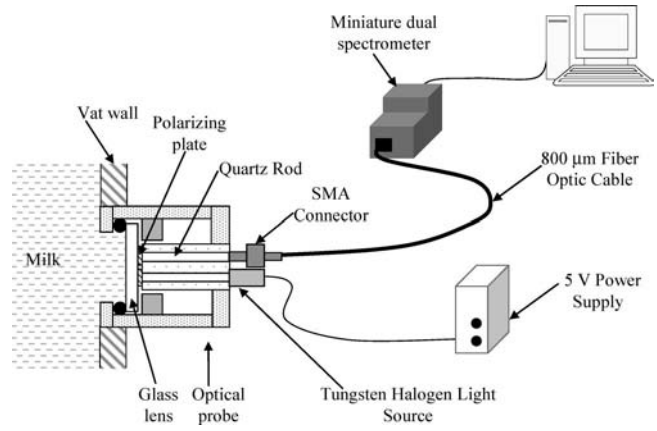

Figure 1. Schematic of the LFV sensor and optical configuration used for monitoring milk coagulation and curd syneresis.

Milk Coagulation. On the day of coagulation trials the milk was adjusted to a final pH of 6.5 at 2 °C using 1.0 M HCl. A constant dilution rate was ensured by adding deionized water for a total added volume of HCl plus deionized water of 60 mL. Milk was slowly heated to the coagulation temperature ± 0.15 °C, to minimize the impact of the temperature change on casein micelle equilibrium. Seven kilograms of the heated milk was added to the vat and left to equilibrate until thermal equilibrium was achieved. Coagulation temperature was controlled using a single-jacket cheese vat supplied with temperature-controlled water through a copper coil connected to a water bath having a control accuracy of ±0.01 °C (Lauda, RM 20, Brinkman Instrument Inc., Westbury, NY). Milk temperature was measured with a precision thermistor (model 5831 A, Omega Engineering, Stamford, CT; resolution ± 0.01 °C; accuracy ± 0.2 °C). The enzyme used for milk coagulation was chymosin (CHY-MAX Extra; EC 3.4.23.4 isozyme B, 643 IMCU mL^{-1}; Chr. Hansen Inc., Milwaukee, WI). Once thermal equilibrium was achieved, chymosin was added to the milk in the vat at a level of 0.06 mL kg^{-1} of milk. Data acquisition for the CL and LFV sensors commenced upon addition of the enzyme, that is, time $t_{c(0)}$.

Inline Light Backscatter Monitoring Instrumentation. *CoAguLite Sensor*. As mentioned above, the CL sensor (model 5, Reflectronics Inc., Lexington, KY) was employed to select the different experimental levels of cutting time and also as a reference light backscatter sensor to which the signal from the LFV could be compared. This sensor transmitted near-infrared light at 880 nm through two 600 μm diameter fibers. One fiber transmitted infrared radiation into the milk sample while the other fiber transmitted the radiation scattered by the milk particles to a silicon photodetector. Further details on the CL sensor and data acquisition system were presented by Castillo et al. (*12, 13*). For calibration the sensor was zeroed by excluding light and adjusting the output voltage to 1 V. The sensor gain was calibrated to give a 2 V signal response when placed in the milk sample. Response data were collected every 6 s. Parameters in the text and or tables presented with an asterisk denote that they were calculated from the CL sensor response as distinct from those obtained from the LFV sensor. The initial voltage response (V^*_0) was calculated by averaging the first 10 data points after correction for the 1 V offset. A light backscatter ratio (R^*)was calculated by dividing the sensor output voltage at any time (less the 1 V output) by V^*_0. The first derivative (R'^*) of the light backscatter ratio profile was calculated by conducting linear least-squares regression on the most recently collected 4 min of data. The calculated slope was assigned to the midpoint of the data subset used. The second derivative (R''^*) was calculated in a similar manner but using 60 data points to smooth the R''^* profile.

Large Field of View Sensor. The LFV sensor was a prototype designed at the University of Kentucky. A schematic for the sensor design is shown in **Figure 1**. Light from a tungsten halogen source (spectral range of 360–2000 nm) travels through a quartz rod, a vertical

Table 2. Definition of Optical Parameters Derived from the Light Backscatter Ratio Profiles during Coagulation and Syneresis

parameter	units	definition[a]
t_{max}	min	time to first maximum of R′
t_{cut}	min	time to gel cutting
t_{2max}	min	time to first maximum of R''
t_{2min}	min	time to the minimum of R''
R_{max}	dimensionless	value of R at t_{max}
R_{2max}	dimensionless	value of R at t_{2max}
R_{2min}	dimensionless	value of R at t_{2min}
R_{cut}	dimensionless	value of R at t_{cut}
R'_{max}	min^{-1}	value of R' at t_{max}
R''_{max}	min^{-2}	value of R'' at t_{max}
ΔR_{coag}	percent	% increase in R from $t_{c(0)}$ to $t_{c(cut)}$
ΔR_{syn}	percent	% decrease in R from $t_{s(0)}$ to $t_{s(85)}$

[a] R = light backscatter ratio; R' = first derivative of the light backscatter ratio; R'' = second derivative of the light backscatter ratio; $t_{c(0)}$ = time of enzyme addition; $t_{c(cut)}$ = end of coagulation; $t_{s(0)}$ = start of syneresis; $t_{s(85)}$ = end of syneresis.

polarizer, and a glass window to the sample. The large-diameter glass window allows scattered light to be collected from a large area. A polarizing plate allows for the selective detection of horizontally polarized light. Scattered light is transmitted through another quartz rod, an SMA connector, and a ~800 μm diameter fiber optic cable (Spectran Specialty Optics, Avon, CT) to the master unit of a dual miniature fiber optic spectrometer (model SD2000, Ocean Optics, Inc., Dunedin, FL). Light emerging from the fiber optic cable is processed in the spectrometer, and the data are transferred to a computer through an A/D converter. The master unit had a 25 μm slit, 300 line mm^{-1} diffraction grating with a range of 300–2000 nm, and a detection bandwidth of 200–1100 nm. The unit was equipped with a 2048 pixel linear CCD array silicon detector (Sony ILX 511, Tokyo, Japan) with a response range of 200–1100 nm and a sensitivity of 86 photons per count at 1 s integration time. Spectra were collected over the range of 300–1100 nm with a resolution of 0.7 μm. The integration time was set to 7 s by the computer software (OOIBase, version 1.5, Ocean Optics, Inc.). Each spectral scan was automatically processed by subtracting the dark background spectral scan. Each spectral scan was reduced to 38 averages by dividing them into 20 nm wavebands with mid-wavelengths of $340 + 20n$ ($1 \leq n \leq 38$), giving 38 wavebands in the range (360–1100 nm) and averaging the optical response for the wavelengths constituting each waveband. The voltage readings (sensor output) for the first minute of data were averaged within each waveband to calculate the initial voltage response, V_0. The voltage intensity at every waveband, V, was divided by its corresponding V_0 to obtain the light backscatter ratio, R. The first derivative, R' of the light backscatter ratio profile was calculated by conducting linear least-squares regression on the most recently collected 4 min of data, if t^*_{max} was $\leq$8 min, or the most recently collected 5 min of data, if t^*_{max} was >8 min. This was because the sensor response at low temperatures, that is, those experiments with $t^*_{max} > 8$ min, contained a greater degree of noise and a 5 min interval was required to smooth the R' profile. The calculated slope was assigned to the midpoint of the data subset used. The second derivative (R'') was calculated in a similar manner but using 60 data points to smooth the R'' profile.

Generation of Light Backscatter Parameters. A number of light backscatter parameters were derived from both the LFV and CL sensor responses during coagulation and syneresis. The light backscatter parameters are defined in **Table 2**. The optical parameters derived from the light backscatter profiles during coagulation were defined by Castillo et al. (*13*) and classified as proposed by Castillo et al. (*12*) (**Table 2**).

Cutting Time Selection and Gel Cutting Procedure. Experimental cutting times used in each experiment were selected on the basis of measurements of light backscatter using the CL sensor. The CL sensor gave a real time target value for t_{cut} for each experiment using the following prediction equation proposed by Payne et al. (*14*):

$$t^*_{cut} = \beta t^*_{max} \quad (1)$$

t^*_{max} was the first maximum of R'^* and β was a constant. The range of β values was selected, around a central value of 2.5, on the basis of previous experimental work (*15*) to ensure that the resulting range of cutting times gave a suitable range of gel firmness at cutting. This resulted in β values (1.3, 1.8, 2.5, 3.2, and 3.7), in compliance with the experimental design shown in **Table 1**, to establish the target t^*_{cut} values for the experiment.

When indicated by the CL data acquisition software, the gel was cut by pushing a cutting knife vertically through the gel. This cut the gel into prismatic columns. The knife was then rotated once, ensuring all of the gel was cut into cubes of approximately 1 cm^3. The last recorded time point prior to cutting is designated $t_{c(cut)}$, with the next time point defined as the start of the syneresis process ($t_{s(0)}$). The curd was left to heal for 4.5 min before stirring at 10 ± 0.02 rpm was initiated (Servodyne mixer 50003-10, Cole Parmer Instrument Co., Chicago, IL). The stirring process continued at this speed for 85 min ($t_{s(85)}$). The practice of heating the vat contents was not simulated as this was outside the scope of the experiment.

Sampling and Compositional Analysis of Curd and Whey. Sampling and compositional analysis of curd and whey were carried out by using previously reported procedures (*15*). Samples of curd and whey were removed for compositional analysis at $t_{s(5)}$ and every 10 min thereafter up to $t_{s(85)}$ (i.e., nine samples). Curd and whey were separated using a sieve (75 μm pore size). Three grams of curd and 5 g of whey were weighed into dishes using an analytical balance. The dishes were dried in a convection oven at 102 °C, until they reached a constant weight (~15 h). Samples were analyzed in triplicate. Chemical composition of whey was also determined using the Milko-Scan FT120.

Syneresis Kinetics. *Curd Moisture Kinetics.* A number of authors have observed that the expulsion of whey from rennet-induced milk gels follows first-order kinetics (*5*, *16–18*). Castillo et al. (*19*) showed that in milk coagulated by a combination of bacterial fermentation and chymosin, whey separation and curd shrinkage followed first-order kinetics. Therefore, the following first-order equation was fitted to the curd moisture experimental data during syneresis:

$$CM_t = CM_\infty + (CM_0 - CM_\infty)\ e^{-k_{CM}t} \quad (2)$$

CM_t was the curd moisture (%) at time t (min), CM_∞ was the curd moisture (%) at an infinite time, CM_0 was the curd moisture content (%) at the beginning of syneresis, $t_{s(0)}$, that is, the milk moisture content, and k_{CM} was the kinetic rate constant (min^{-1}) for curd moisture content changes during syneresis. Procedure NLIN in SAS was used to determine the parameters CM_∞ and k_{CM}, whereas CM_0 was set at the known value for the milk moisture content in each experiment.

Whey Fat Concentration Kinetics. Castillo et al. (*20*) found that during industrial cheesemaking whey fat concentration in the vat followed a first-order response. As will be discussed under Results and Discussion, temperature affects whey fat release during syneresis. At temperatures below 37 °C whey fat concentration decreased during syneresis, but at 37 °C or higher whey fat concentration increased during syneresis. Therefore, two equations were required to characterize the change in whey fat concentration during syneresis. At temperatures below 37 °C whey fat concentration was fitted to a first-order decreasing equation

$$WF_t = WF_\infty + (WF_5 - WF_\infty)\ e^{-k_{WF}t} \quad (3)$$

whereas at temperatures of 37 °C or higher a first-order increasing equation was used

$$WF_t = WF_5 + (WF_\infty - WF_5)(1 - e^{-k_{WF}t}) \quad (4)$$

where WF_t was the whey fat concentration (%) at time t (min), WF_∞ was the whey fat content (%) at an infinite time, WF_5 was the whey fat content (%) 5 min after cutting time, $t_{s(5)}$, and k_{WF} was the kinetic rate constant (min^{-1}) for whey fat concentration changes during syneresis (we will use the term whey fat dilution to describe the changes of whey fat concentration during syneresis). Procedure NLIN was used to predict the parameters WF_∞, WF_5, and k_{WF}.

LFV Sensor Response Kinetics. If we expect the signal from the LFV sensor to be related to curd moisture or whey fat concentration

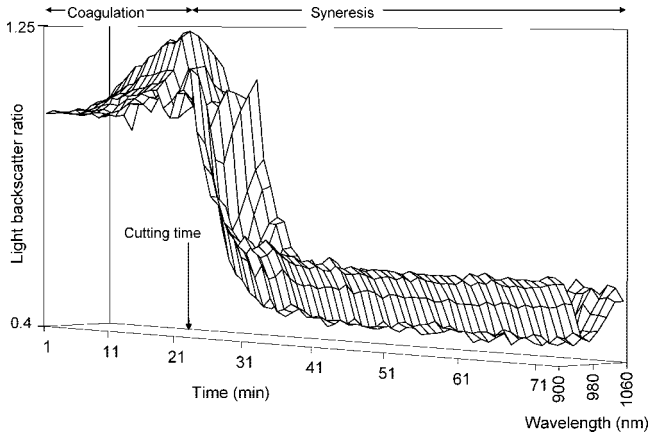

Figure 2. Typical LFV sensor response (average of three replicates) during coagulation and syneresis (temperature = 32 °C; $CaCl_2$ = 2 mM) at wavelengths between 900 and 1060 nm. Time is measured from rennet addition (time = 0 min).

or both, the signal should follow first-order kinetics for most conditions, except for high-temperature conditions, at which the signal may reflect the particular effect of temperature on whey fat content. Therefore, the LFV sensor response during syneresis was also fitted to a first-order equation as

$$R_t = R_\infty + (R_0 - R_\infty)\ e^{-k_{LFV}t} \quad (5)$$

where R_t was the light backscatter ratio at time t (min), R_∞ was the light backscatter ratio at an infinite time, R_0 was the light backscatter ratio at $t_{s(0)}$, and k_{LFV} was the kinetic rate constant (min^{-1}) for the LFV sensor response during syneresis. Procedure NLIN was used to predict the parameters R_∞, R_0, and k_{LFV}.

Statistical Analysis. The experimental data recorded for curd moisture content, whey fat content, and LFV sensor response as a function of time during syneresis was fitted using the Proc NLIN procedure in SAS. The significance of the relationships between parameters was explored using the Proc CORR procedure in SAS.

RESULTS AND DISCUSSION

Compositional analysis of the milk showed that there were minimal differences between batches. The average composition of the milk ± standard deviation (SD) was 3.7 ± 0.3, 3.5 ± 0.1, and 12.2 ± 0.3% for fat, protein, and total solids contents, respectively.

LFV Sensor Spectral Response. A typical light backscatter profile derived from the LFV sensor during coagulation and syneresis at wavelengths between 900 and 1060 nm is shown in **Figure 2**. During coagulation the light backscatter ratio increased, and the LFV sensor response was greatest at 980 nm as indicated by the peak at this wavelength observed throughout coagulation (**Figure 2**). With the onset of syneresis following cutting of the gel, the signal decreased exponentially over time. **Figure 2** also shows that the LFV sensor response during syneresis was further characterized by a valley at 980 nm. This trend, of a maximum increase during coagulation and the maximum decrease during syneresis at 980 nm, was consistently observed for all experimental conditions. For all conditions the average increase during coagulation at 980 nm was 20.5 ± 5.8% (mean ± SD), whereas during syneresis the average decrease was 59.4 ± 12.0% (mean ± SD). Generally the LFV sensor signal also incorporated less noise at 980 nm than at other wavelengths. On this basis the following analysis of the LFV sensor response has been carried out at 980 nm.

LFV Sensor Response to Coagulation. Figure 3 compares the response of the LFV sensor (960, 980, 1000 nm) during coagulation and syneresis to that of the CL sensor (880 nm) at three different temperatures. Each profile is an average of three replicates. In general the CL sensor produced a smoother response during coagulation than the LFV sensor. However, both sensors did respond in a similar manner. The CL sensor response increased during coagulation by 26.5 ± 8.0% (mean ± SD), which was comparable to that of the LFV sensor (20.5 ± 5.8%). It is known that changes in the light-scattering properties of milk undergoing enzymatic coagulation are caused by changes in the molecular weight, size, and number of colloidal casein micelle aggregates (*21*). Ustunol et al. (*22*) divided the light-scattering profile of enzymatically coagulated milk into three periods, induction, sigmoidal, and logarithmic, which related to the different stages of coagulation, namely, enzymatic hydrolysis of κ-casein, aggregation of casein, and cross-linking.

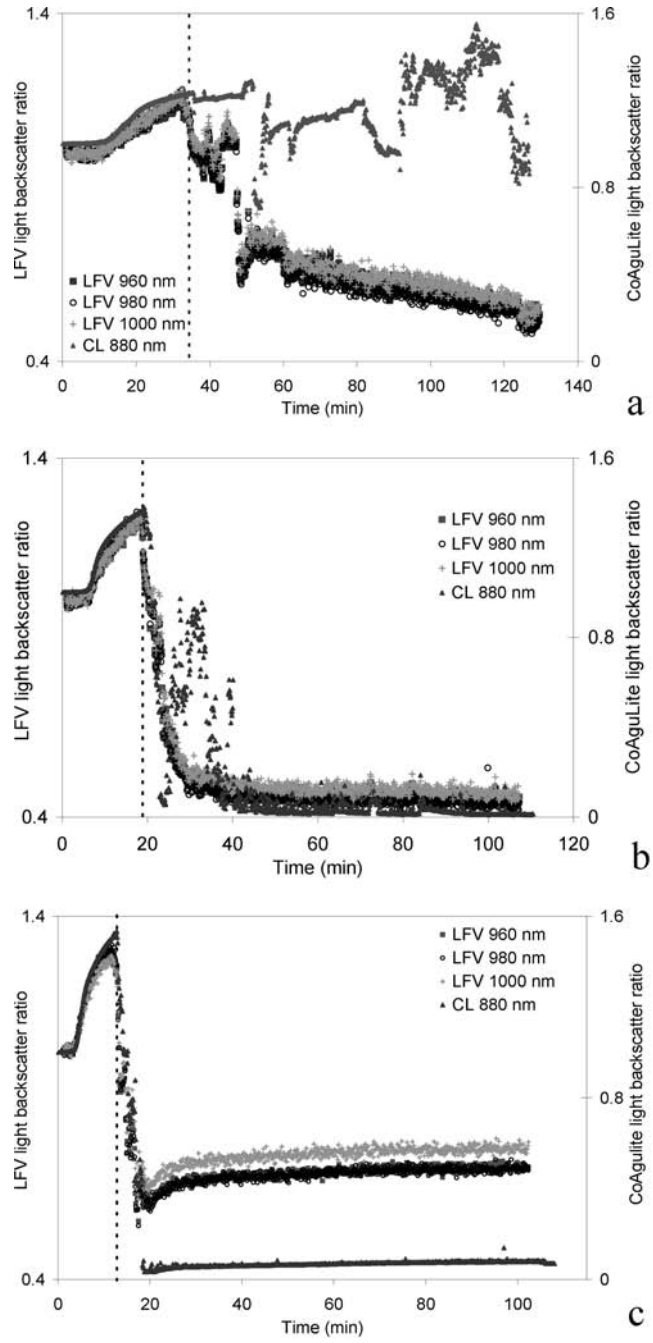

Figure 3. Average of three LFV sensor profile replicates under constant β and $CaCl_2$ addition levels (β = 2.5, $CaCl_2$ = 2 mM) and increasing temperature: (**a**) 23.6 °C; (**b**) 32.0 °C; (**c**) 40.4 °C.

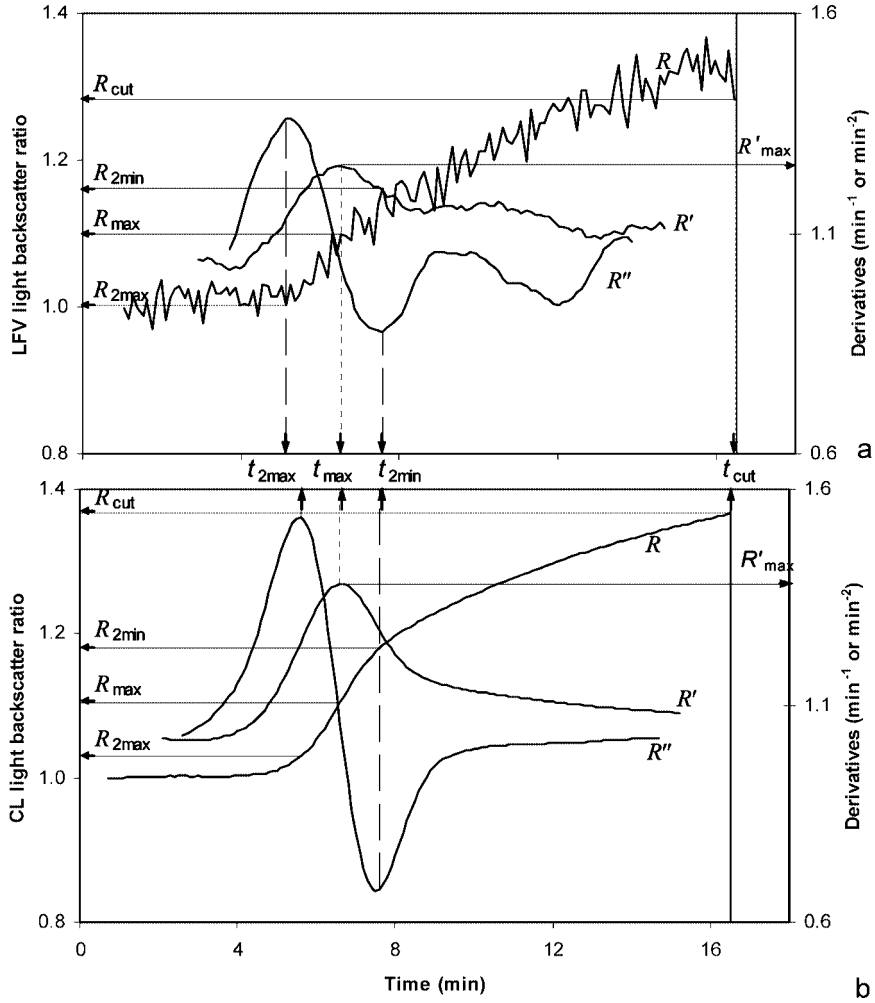

Figure 4. Light backscatter ratio profiles and their characteristic first and second derivatives versus time for the (**a**) LFV sensor and (**b**) CL sensor (temperature = 32 °C, β = 2.5, $CaCl_2$ = 2 mM).

Milk coagulation is highly dependent on temperature (*23*), and Payne et al. (*14*) reported that temperature affected the shape of the light backscatter profile of milk undergoing enzymatic coagulation. This is due to temperature affecting both the rate of enzymatic hydrolysis and the rate of network assembly (i.e., casein aggregation and gel firming) (*24*). The effect of temperature on the sensor responses is illustrated in **Figure 3**. Increasing the temperature is known to decrease the gelation time (*12*, *23*), and this was observed as a shorter induction period at the start of the coagulation profile at higher coagulation temperatures (**Figure 3**), smaller time parameters (t_{max}, t_{2max}, t_{2min}), and higher R'_{max} value. This corresponds with a higher rate of enzymatic hydrolysis of κ-casein and hence a faster onset and rate of aggregation and curd firming. Temperature was also found to significantly increase the light backscatter ratio of the LFV and CL sensors at cutting time ($P \leq 0.0001$). Presumably this is due to the greater rate of aggregation. This is in agreement with previously reported results (*12*). Castillo et al. (*24*) attributed the light backscatter ratio profile after t^*_{max} to a combination of casein micelle aggregation and curd firming. They also found aggregation and curd-firming rate constants increased with increasing temperature.

To determine if the LFV sensor is comparable to the CL sensor for monitoring coagulation, optical parameters, as defined in **Table 2**, were derived from the LFV and CL light backscatter ratio profiles during coagulation. **Figure 4** shows the LFV and CL response to coagulation and their respective derivatives. It is clear the LFV sensor response contains a high degree of scatter, which could present a difficulty in calculating important parameters such as t_{max}. Despite the degree of noise in the light backscatter ratio, R, it was still possible to successfully calculate R' and R'' and derive the same parameters as listed in **Table 2** that were derived from the CL sensor response and which can be used to characterize coagulation. Correlations between the CL- and LFV-derived parameters are shown in **Table 3**. These results demonstrate the close relationship between the CL- and LFV-derived parameters obtained during milk coagulation. All LFV-derived parameters were significantly correlated with CL-derived parameters. In particular, the LFV parameters, t_{max}, t_{2max}, t_{2min}, and R'_{max} were very significantly correlated with their CL-derived counterparts [correlation coefficient (r) = 0.96–0.99, $P \leq 0.001$]. Considering the level of scattering in R the correlation between R_{max} and R^*_{max} is still reasonable and significant ($r = 0.63$, $P < 0.001$). Parameters t_{max}, t_{2max}, and t_{2min} were all found to be significantly correlated (r = 0.96–0.99, $P \leq 0.001$), which compares favorably with data presented by Castillo et al. (*13*), who noted that the response of such time parameters to temperature was identical and the correlations between them were highly significant ($r = 0.99$, $P < 0.001$). The parameters t_{max} and R'_{max} are dependent on coagulation rate (*12*) and, as expected, were found to be significantly and negatively correlated ($r = -0.89$, $P < 0.001$). Castillo et al. (*25*) also found that an increased coagulation rate (R'_{max}) resulted in a decreased t_{max} ($r = -0.61$, $P < 0.01$).

These results strongly suggest that the LFV sensor, which has a wider field of view, is sensitive, like the CL sensor, to

Table 3. Pearson Correlation Coefficients (r) and Significance[a] between Parameters Derived from the LFV and CL Sensors Coagulation Profile

	t_{2max}	t_{2min}	R_{max}	R'_{max}	t^*_{max}	t^*_{2max}	t^*_{2min}	R^*_{max}	R'^*_{max}
t_{max}	0.97***	0.98***	−0.41**	−0.89***	0.99***	0.99***	0.99***	−0.76***	−0.89***
t_{2max}	1	0.96***	−0.44***	−0.89***	0.97***	0.96***	0.97***	−0.76***	−0.90***
t_{2min}		1	−0.38**	−0.83***	0.99***	0.97***	0.99***	−0.68***	−0.83***
R_{max}			1	0.63***	−0.46***	−0.47***	−0.46***	0.63***	0.62***
R'_{max}				1	−0.89***	−0.92***	−0.89***	0.89***	0.97***
t^*_{max}					1	0.99***	1.00***	−0.76***	−0.89***
t^*_{2max}						1	0.99***	−0.79***	−0.92***
t^*_{2min}							1	−0.76***	0.90***
R^*_{max}								1	0.94***

[a] Significance: ***, $P < 0.001$; **, $P < 0.01$. $N = 60$. Parameters in the text or tables superscripted with an asterisk were calculated from the CL sensor response as distinct from those obtained from the LFV sensor.

both aggregation of casein micelles and the development of curd firmness. Therefore, the LFV sensor has the potential to monitor milk coagulation. However, further modification of its design is recommended to reduce the level of noise to a more acceptable level.

LFV Sensor Response to Syneresis. The most novel aspect of the LFV sensor is its potential to monitor syneresis. **Figure 3** shows that upon cutting of the milk gel there is a sharp decrease in the light backscatter ratio profile of the LFV sensor at all temperatures. In contrast, the CL sensor profile during syneresis was found to be erratic with the exception of the CL profiles derived at 40.4 °C. At this temperature, scatter in the CL response was minimal and it produced a profile similar to that given by the LFV sensor. However, at 40.4 °C the LFV sensor response shows a clearly defined increase in the light backscatter ratio following the initial decrease upon cutting. This is only faintly observed in the CL sensor response. As the LFV sensor provided better defined responses at all temperatures than the CL sensor, the wider field of view was successful in achieving its objective of providing a more representative view of the curd/whey mixture.

Figure 3 shows that the decrease in the LFV sensor response during syneresis is clearly affected by temperature. The parameter ΔR_{syn}, defined in **Table 2** as the percent decrease in R from $t_{s(0)}$ to $t_{s(85)}$, was derived from the response of R during syneresis. It provides a measure of the magnitude of the decrease in the signal during syneresis. Increasing the temperature from 23.6 to 32 °C increased ΔR_{syn}; the decrease in ΔR_{syn} also appears to occur more rapidly at 32 °C than at 23.6 °C (**Figure 3a**,**b**). This trend also appeared at 40.4 °C; however, at approximately 20 min (**Figure 3c**) R begins to increase again. The unexpected response observed in R at 40.4 °C was also seen at 37 °C, although it was less pronounced. We hypothesize that the varying response of R at different temperatures may be a result of compositional changes in whey or shrinkage of curd. Although the relationship between optical changes and the process of coagulation is well documented, the relationship between optical changes recorded by the LFV sensor and the process of syneresis is unknown. However, it has been documented by many authors that the kinetics of syneresis follows first-order reactions such as the kinetics of whey expulsion, curd shrinkage, and fat losses (*5, 16–18, 20*). Therefore, if R is related to changes occurring during syneresis, it should most likely follow first-order kinetics.

Thus, curd moisture content at 10 min intervals was fitted to eq 2, whey fat content at 10 min intervals for experiments carried out at 23.6–32 °C and 37–40.4 °C was fitted to eqs 3 and 4, respectively, and R from $t_{s(0)}$ was fitted to eq 5. The R^2 values between the experimental and fitted data are shown in **Table 4**.

For the fitting of curd moisture, R^2 was between 0.98 and 1.00 (**Table 4**), indicating that changes in curd moisture content during syneresis follows first-order kinetics. Panels **a**, **b**, and **c** of **Figure 5** show graphically the fitting of eq 2 to curd moisture experimental data for milk coagulated at 23.6, 32, and 40.4 °C, respectively. The kinetic rate constant (min^{-1}) for curd moisture content changes during syneresis, k_{CM}, was found to be in the range of 0.06 ± 0.03 min^{-1} (mean ± SD) for all experimental conditions. This is of the same order of magnitude as the kinetic rate constants reported for the expulsion of whey from rennet-induced skim milk gels (*26*) and rennet-induced goat's milk gels (*18*). Both k_{CM} and CM_∞ [curd moisture (%) at an infinite time], were affected by temperature. k_{CM} increased and CM_∞ decreased with increasing temperature. The temperature coefficients (Q_{10}) for changes in curd moisture content at 1 and 2 mM calcium chloride addition level (CCAL) were 1.95 and 2.33, respectively. This compares favorably with the Q_{10} reported for rennet-induced skim milk gels (*26*). The Arrhenius plot [$\ln(k_{CM})$ against $1/T$ (K^{-1})] was used to estimate the activation energy (E_a) for curd whey expulsion during syneresis. E_a values for whey expulsion were 54.1, 66.5, and 67.7 kJ/mol for 1, 2, and 3 mM CCAL, respectively. Although E_a appeared to increase with increased CCAL, this was not found to be significant. Walstra et al. (*4*) noted that the main effect of $CaCl_2$ addition is a reduction in milk pH, which increases syneresis.

Table 4. Coefficients of Determination (R^2) between Experimental Data and Predicted Values for Curd Moisture Content, Whey Fat, and the LFV Sensor Response at Various Renneting Temperatures

temperature (°C)	N	curd moisture content (eq 2)	whey fat content (eq 3 or 4)	LFV sensor (eq 1)	LFV sensor DM[a] (eqs 5 and 6)
23.6	3	0.97	0.99	0.76	
27	12	0.95	1.00	0.93	
32	30	0.96	0.98	0.96	
37	12	0.97	0.99	0.87	0.90
40.4	3	0.94	0.99	0.72	0.83

[a] DM, large field view dual model, see text.

Castillo et al. (*27*) suggested that whey fat could act as an internal tracer of whey expulsion during syneresis as most fat is released upon cutting of the milk gel. Whey continues to be expelled over time, and hence whey fat will be diluted. Temperature was clearly found to affect the kinetics of whey fat dilution over time as expressed by the need for two different first-order equations (eqs 3 and 4). The fit of these equations was found to be excellent, with R^2 of 0.98–1.0 between the experimental and fitted data (**Table 4**), showing that changes in whey fat content during syneresis followed first-order kinetics. As shown in **Figure 5d**,**e**, at temperatures of 23.6–32 °C, whey fat was diluted over time as expected. However, at 37 and 40.4 °C, as illustrated in **Figure 5f**, the

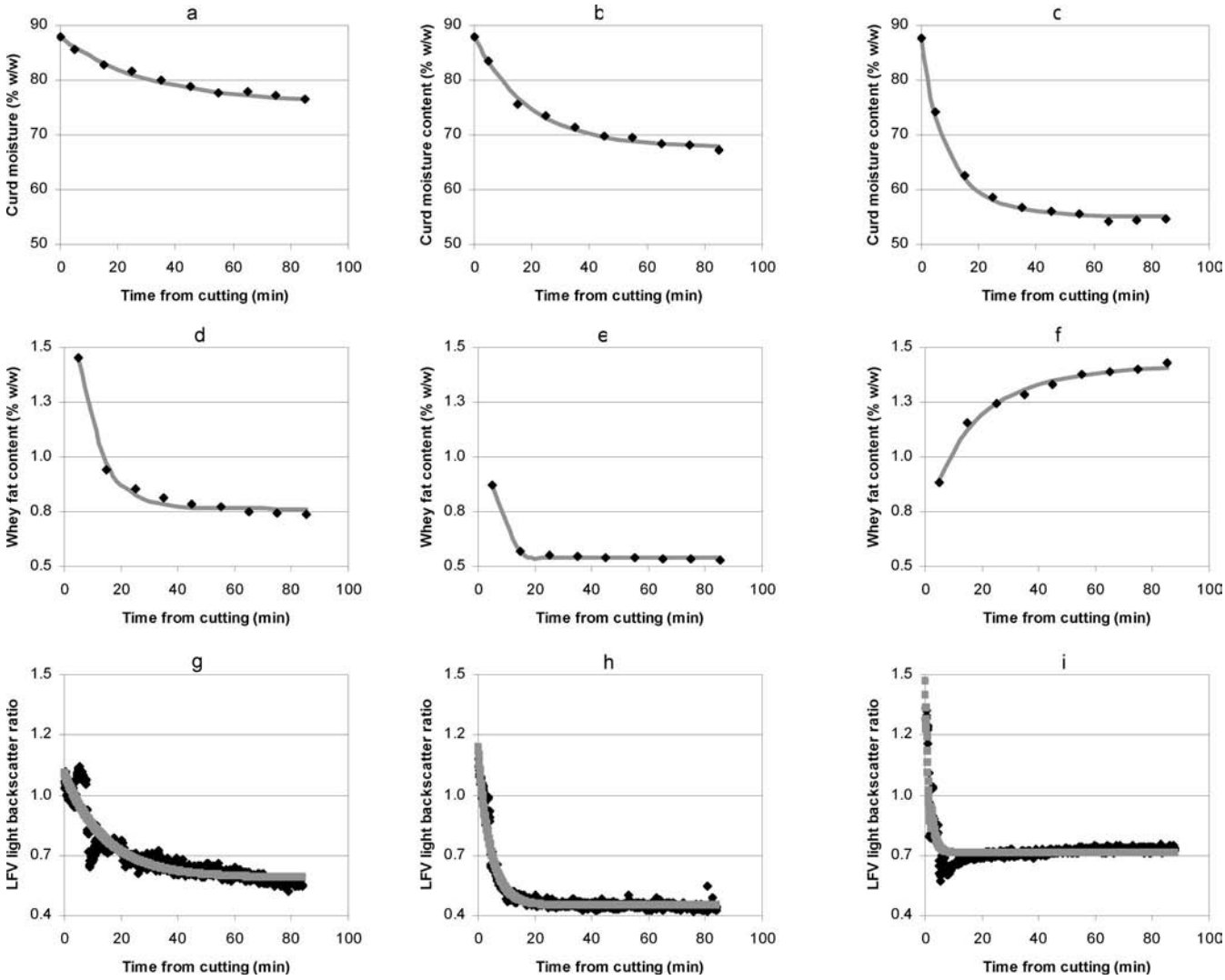

Figure 5. Kinetics of curd moisture content (**a**–**c**), whey fat content (**d**–**f**), and LFV light backscatter ratio (**g**–**i**) as a function of time during syneresis at 23.6 °C (**a**, **d**, **g**), 32.0 °C (**b**, **e**, **h**), and 40.4 °C (**c**, **f**, **i**) under constant β and $CaCl_2$ addition levels ($\beta = 2.5$, $CaCl_2 = 2$ mM). Time zero corresponds to the cutting time. Theoretical curve (—) assuming first-order kinetics (eq 2, 3, 4, or 5). The average value of the experimental data (♦) at the test conditions is shown ($n = 3$).

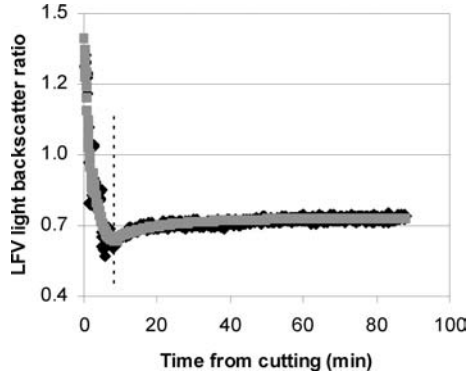

Figure 6. Kinetics of the LFV light backscatter ratio as a function of time during syneresis at 40.4 °C under constant β and $CaCl_2$ addition levels ($\beta = 2.5$, $CaCl_2 = 2$ mM). Time zero corresponds to the cutting time. The dashed line indicates the point at which the sensor response was split. The solid line is the theoretical curve assuming first-order kinetics (eqs 5 and 6). The average value of the experimental data (♦) at the test conditions are shown ($n = 3$).

concentration of whey fat increased over time, indicating that at these temperatures there is continuous release of whey fat. We suggest that because whey fat has a general melting point of 37 °C (*28*), the mobility of the fat globules at this temperature increases, allowing them to be expelled throughout syneresis and not just upon cutting of the gel. Temperature also affected the level of fat losses. The whey fat content (percent) at $t_{s(5)}$, (WF_5) decreased significantly as the temperature increased between 23.6 and 32 °C ($P < 0.0001$); however, no significant difference in WF_5 was observed between 32 and 40.4 °C. Temperature, however, had a different effect on whey fat content at an infinite time (WF_∞). As observed for WF_5, increasing temperature from 23.6 to 32 °C decreased WF_∞ significantly ($P < 0.0001$), whereas increasing temperature from 32 to 40.4 °C significantly increased WF_∞ ($P < 0.0001$). The kinetic rate constant for whey fat dilution (k_{WF}) increased significantly between 23.6 and 32 °C ($P < 0.002$), but no significant difference in k_{WF} was detected between 37 and 40.4 °C. Similar trends (results not shown) were obtained for total solids as for whey fat content, indicating that total solids of whey were dominated by whey fat.

The correlation between the experimentally recorded R and R fitted using eq 5 is shown in **Table 4**. At 27 and 32 °C the correlation was very strong (R^2 of 0.93 and 0.95, respectively). The R^2 for the fit at 23.6 °C is lower ($R^2 = 0.76$), mainly due

Table 5. Correlation Coefficients (r) and Significance[a] between Parameters Derived from the LFV Sensor Profile and Kinetic Parameters

	ΔR_{coag} (%)	ΔR_{syn} (%)	k_{CM}	k_{WF}	k_{LFV}
t_{max}	−0.19ns	0.01ns	−0.58***	0.11ns	−0.60***
t_{2max}	−0.14ns	0.10ns	−0.58***	0.17ns	−0.63***
t_{2min}	−0.20ns	−0.03ns	−0.52***	0.03ns	−0.54***
R_{max}	0.12ns	−0.39**	0.43***	−0.24ns	0.47***
R_{2min}	0.24ns	−0.43***	0.54***	−0.42**	0.65***
R_{2max}	0.19ns	0.02ns	0.48**	−0.14ns	0.67***
R'_{max}	0.15ns	−0.23ns	0.67***	−0.37**	0.76***
ΔR_{coag} (%)	1	0.03ns	−0.003ns	0.2ns	0.15ns
ΔR_{syn} (%)		1	−0.24ns	0.45***	−0.41**
k_{CM}			1	−0.27*	0.84***
k_{WF}				1	0.42**
k_{LFV}					1

[a] Significance: ***, $P < 0.001$; **, $P < 0.01$; *, $P < 0.05$; ns, not significant. $N = 60$.

to the greater degree of scatter in R at lower temperatures as previously mentioned. This indicates that R did follow a first-order decrease upon cutting at these temperatures. However, the response of R during syneresis, at 37 and 40.4 °C, was complicated by R decreasing followed by a subsequent increase as observed in **Figure 3c**. The inability of eq 5 to account for the subsequent increase in R is reflected in the lower R^2 values shown in **Table 4** for 37 and 40.4 °C ($R^2 = 0.87$ and 0.72) and illustrated graphically in **Figure 5i**. It is suggested that if whey fat is acting as an internal tracer that the LFV sensor is monitoring, then the lack of fit of R to first-order kinetics at 37 and 40.4 °C is related to the continuous expulsion of fat from the curd at these temperature as observed in **Figure 5f**. To investigate this possibility R recorded at 37 and 40.4 °C was split into two sections, that is, before and after the time at which R began to increase. The first section continued to be fitted using eq 5, whereas the second section was fitted to eq 6, which is based on an increasing first-order kinetic equation, as was used in eq 4 for whey fat content.

$$R_t = R_0 + (R_\infty - R_0)(1 - e^{-k_{LFV}t}) \quad (6)$$

where R_t was the light backscatter ratio during syneresis at time t (min), R_∞ was the light backscatter ratio at an infinite time, R_0 was the light backscatter ratio at $t_{s(0)}$, and k_{LFV} was the kinetic rate constant (min^{-1}) for the LFV sensor response during syneresis. The combination of fitting eqs 5 and 6 was denoted as the LFV dual model (DM). The fitting of the DM is shown graphically in **Figure 6**. When compared with **Figure 4i**, which shows the same experimental data, **Figure 6** clearly shows that a better fit was obtained using the DM at 40.4 °C (**Figure 6**) than was obtained by using eq 5 (**Figure 4i**). The R^2 values for the DM are given in **Table 4**. Splitting R into two sections and fitting them separately improved the fit, with R^2 values of 0.90 and 0.83 for 37 and 40.4 °C respectively.

Table 5 shows the correlation between kinetic and optical parameters derived from the LFV sensor during coagulation and syneresis. Interestingly, k_{CM} is significantly correlated with all of the coagulation parameters, suggesting that the rate of whey expulsion from the curd (i.e., curd shrinkage) is primarily determined by conditions during coagulation. However, k_{WF} was only significantly correlated with two coagulation parameters, but unlike k_{CM}, it was significantly correlated with ΔR_{syn}, suggesting that the rate of whey fat loss is dependent to some extent on both coagulation and syneresis conditions. k_{LFV} was found to be significantly related to both coagulation and syneresis parameters, but most significantly k_{LFV} was significantly correlated with k_{CM} ($r = 0.84$, $P < 0.001$) and k_{WF} ($r = 0.42$, $P < 0.01$). Although the correlation between k_{WF} and k_{LFV} was weak, it should be noted that k_{WF} was derived from the original fitting of R to eq 5, which does not fully account for the response of R at high temperatures. These results indicate that the response of the LFV sensor during syneresis is related to changes in curd moisture content and whey fat content.

Table 6. Correlation Coefficients (r) and Significance[a] between the Average or Predicted Light Backscatter Ratio at Sampling and Curd Moisture or Whey Fat Content

	temperature (°C)	N	curd moisture	whey fat
R_{av10}	23.6	3	0.81***	0.92***
R_{av10}	27	12	0.72***	0.67***
R_{av10}	32	30	0.83***	0.85***
R_{av10}	37	12	0.47***	0.76***
R_{av10}	40.4	3	0.67***	0.87***
	all temperatures	60	0.58***	0.74***
R (eq 5)	23.6	2	0.84***	0.95***
R (eq 5)	27	12	0.71***	0.73***
R (eq 5)	32	30	0.85***	0.82***
R (eqs 5 and 6)	37	12	0.84***	0.77***
R (eqs 5 and 6)	40.4	3	0.69***	0.75***
	all temperatures	60	0.57***	0.77***

[a] Significance: ***, $P < 0.001$; **, $P < 0.01$; *, $P < 0.05$; ns, not significant.

To further confirm this, the correlation between R and both curd moisture and whey fat content at each sampling point was investigated. At each sampling point it was necessary to move the lid of the vat to remove a sample, allowing external light to enter the vat, which could cause some minor interference in R. To overcome this, the last five measurements of R prior to sampling (28 s) and the subsequent five measurements of R (28 s) were averaged. This value was denoted R_{av10}. The correlation between R_{av10} and curd moisture and whey fat content is shown in **Table 6**. **Table 6** also shows the correlation between the predicted R derived using either eq 5 (23.6–32 °C) or the dual model using both eqs 5 and 6 (37–40.4 °C). The strong significant relationships observed between R_{av10} or the predicted R values and both curd moisture and whey fat content further indicate that the LFV sensor is sensitive to changes in curd moisture and whey fat content and could therefore be developed as a sensor for monitoring syneresis.

In conclusion, the results of this study show that the LFV sensor is sensitive to both aggregation of casein micelles and development of curd firmness and that the sensor response during syneresis is related to changes in curd moisture and whey fat content. The effect of temperature on the sensor response was also found to be consistent with the effect of temperature on the kinetics of both coagulation and syneresis. Therefore,

the prototype LFV sensor has potential for continuous monitoring of both coagulation and syneresis during cheesemaking, and the results of this study should be validated at pilot scale to facilitate the study of the LFV sensor using standard industrial cheesemaking practices.

LITERATURE CITED

(1) Pearse, M. J.; Mackinlay, A. G. Biochemical aspects of syneresis: a review. *J. Dairy Sci.* **1989**, *72* (6), 1401–1407.

(2) Lawrence, R. C.; Gilles, J. The assessment of the potential quality of young Cheddar cheese. *N. Z. J. Dairy Sci. Technol.* **1980**, *15* (1), 1–12.

(3) Daviau, C.; Pierre, A.; Famelart, M.-H.; Goudedranche, H.; Jacob, D.; Garnier, M.; Maubois, J.-L. Characterisation of whey drainage kinetics during soft cheese manufacture in relation with the physicochemical and technological factors,pH at renneting, casein concentration and ionic strength of milk. *Lait* **2000**, *80*, 417–432.

(4) Walstra, P.; Dijk, H. J. M. V.; Geurts, T. J. The syneresis of curd, 1. General considerations and literature review. *Neth. Milk Dairy J.* **1985**, *39*, 209–246.

(5) Marshall, R. An improved method for measurement of the syneresis of curd formed by rennet action on milk. *J. Dairy Res.* **1982**, *49*, 329–336.

(6) Johnston, K. A.; Luckman, M. S.; Lilley, H. G.; Smale, B. M. Effect of various cutting and stirring conditions on curd particle size losses of fat to the whey during Cheddar manufacture in ost vats. *Int. Dairy J.* **1998**, *8*, 281–288.

(7) Lawrence, A. J. Syneresis of rennet curd. Part 2. Effect of stirring and of the volume of whey. *Aust. J. Dairy Technol.* **1959**, *14* (4), 169–72.

(8) Zviedrans, Z.; Graham, E. R. B. An improved tracer method for measuring the syneresis of rennet curd. *Aust. J. Dairy Technol.* **1981**, 117–120.

(9) Nilsen, K. O.; Abrahamsen, R. K. Difficulties in measuring the syneresis of goat milk rennet curd by dilution of an added tracer. *J. Dairy Res.* **1985**, *52* (1), 209–212.

(10) Taifi, N.; Bakkali, F.; Faiz, B.; Moudden, A.; Maze, G.; D. D. Characterization of the syneresis and the firmness of the milk gel using an ultrasonic technique. *Meas. Sci. Technol* **2006**, *17* (2), 281–287.

(11) Tellier, C.; Mariette, F.; Guillement, J.-P.; Marchel, P. Evolution of water proton muclear magnetic relaxation during milk coagulation and syneresis:structural implications. *J. Agric. Food Chem.* **1993**, *41*, 2259–2266.

(12) Castillo, M.; Payne, F. A.; Hicks, C. L.; Lopez, M. B. Predicting cutting and clotting time of coagulating goat's milk using diffuse reflectance: effect of pH, temperature and enzyme concentration. *Int. Dairy J.* **2000**, *10* (8), 551–562.

(13) Castillo, M.; Lucey, J. A.; Payne, F. A. The effect of temperature and inoculum concentration on rheological and light scatter properties of milk coagulated by a combination of bacterial fermentation and chymosin. Cottage cheese-type gels. *Int. Dairy J.* **2006**, *16* (2), 131–146.

(14) Payne, F. A.; Hicks, C. L.; Madangopal, S.; Shearer, S. A. Fiber optic sensor for predicting the cutting time of coagulating milk for cheese production. *Trans. ASAE* **1993**, *36* (3), 841–847.

(15) Fagan, C. C.; Leedy, M.; Castillo, M.; Payne, F. A.; O'Donnell, C. P.; O'Callaghan, D. J. Development of a light scatter sensor technology for on-line monitoring of milk coagulation and whey separation. *J. Food Eng.* **2007**, *83* (1), 61–67.

(16) Peri, C.; Lucisano, M.; Donati, E. Studies on coagulation of milk ultrafiltration retentates II. Kinetics of whey syneresis. *Milchwissenschaft* **1985**, *40* (11), 650–652.

(17) Weber, F. El desuerado del coágulo. In *El Queso*; Eck, A., Ed.; Omega, S. A.: Barcelona, Spain, 1989.

(18) Castillo, M.; Jordan, M. J.; Godoy, A.; Laencina, J.; Lopez, M. B. Kinetics of syneresis in fresh goat cheese. *Milchwissenschaft* **2000**, *55* (10), 566–569.

(19) Castillo, M.; Lucey, J. A.; Wang, T.; Payne, F. A. Effect of temperature and inoculum concentration on gel microstructure, permeability and syneresis kinetics: cottage cheese-type gels. *Int. Dairy J.* **2006**, *16* (2), 153–163.

(20) Castillo, M.; Payne, F. A.; Lopez, M. B.; Ferrandini, E.; Laencina, J. Preliminary evaluation of an optical method for modeling the dilution of fat globules in whey during syneresis of cheese curd. *Appl. Eng. Agric.* **2005**, *21* (2), 265–268.

(21) McMahon, D. J.; Brown, R. J.; Ernstrom, C. A. Enzymic coagulation of milk casein micelles. *J. Dairy Sci.* **1984**, *67* (4), 745–748.

(22) Ustunol, Z.; Hicks, C. L.; Payne, F. A. Diffuse reflectance profiles of 8 milk-clotting enzyme preparations. *J. Food Sci.* **1991**, *56* (2), 411–415.

(23) O'Callaghan, D. J.; Mulholland, E. P.; Duffy, A. P.; O'Donnell, C. P.; Payne, F. A. Evaluation of hot wire and optical sensors for on-line monitoring of curd firmness during milk coagulation. *Ir. J. Agric. Food Res.* **2001**, *40* (2), 227–238.

(24) Castillo, M. Z.; Payne, F. A.; Hicks, C. L.; Laencina, J. S.; Lopez, M.-B. M. Modelling casein aggregation and curd firming in goats' milk from backscatter of infrared light. *J. Dairy Res.* **2003**, (70), 335–348.

(25) Castillo, M.; Gonzalez, R.; Payne, E. A.; Laencina, J.; Lopez, M. B. Optical monitoring of milk coagulation and inline cutting time prediction in murcian al vino cheese. *Appl. Eng. Agric.* **2005**, *21* (3), 465–471.

(26) Kaytanli, M.; Erdem, Y. K.; Tamer, I. M. Factors affecting whey drainage rate of renneted skim milk gels: a kinetic approach. *Milchwissenschaft* **1994**, *49* (4), 197–200.

(27) Castillo, M.; Payne, F. A.; Lopez, M. B.; Ferrandini, E.; Laencina, J. Optical sensor technology for measuring whey fat concentration in cheese making. *J. Food Eng.* **2005**, *71* (4), 354–360.

(28) Fox, P. F.; McSweeney, P. L. H. *Advanced Dairy Chemistry*; Springer: New York, 2003; Vol. 2, Lipids.

Received for review March 19, 2007. Revised manuscript received August 9, 2007. Accepted August 18, 2007. Funding for this research was provided by the Irish Department of Agriculture and Food through the Food Institutional Research Measure (FIRM), by the Kentucky Science and Engineering Foundation (Project KSEF-407-RDE-004), and by the U.S. Department of Agriculture (Project NRI-USDA 2005-35503-15390).

JF070807B